

Synthesis of Novel Cinnamides and a Bis Cinnamate Bearing 1,2,3-Triazole Functionalities with Antiproliferative and Antimetastatic Activities on Melanoma Cells

Fabiola S. Santos,^{#a} Juliana A. do Vale,^{#b} Lucas S. Santos,^a Talita B. Gontijo,^a
Graziela D. A. Lima,^b Leandro L. de Oliveira,^b Mariana Machado-Neves,^b
Róbson R. Teixeira^b and Rossimiriam P. de Freitas^b*,^a

^aLaboratório de Síntese Orgânica (LABSINTO), Departamento de Química,
Universidade Federal de Minas Gerais (UFMG), 31270-901 Belo Horizonte-MG, Brazil

^bDepartamento de Biologia Geral, Universidade Federal de Viçosa (UFV), 36570-900 Viçosa-MG, Brazil

^cDepartamento de Química, Universidade Federal de Viçosa (UFV), 36570-900 Viçosa-MG, Brazil

The present investigation describes the synthesis of novel cinnamides and a bis cinnamate bearing 1,2,3-triazole functionalities and investigation of their antiproliferative and antimetastatic effects on melanoma cells. The necessity for the development of new chemotherapeutic agents for melanoma treatment motivated this work. Sixteen derivatives were obtained with yields ranging from 23-81% and fully characterized by spectroscopic (¹H and ¹³C nuclear magnetic resonance, infrared) and spectrometric high resolution mass spectrometry (HRMS) techniques. The derivatives were *in vitro* evaluated against B16-F10 murine melanoma cell line. The most effective compound (a bis cinnamate) (**6b**) reduced the melanoma cell viability, generated cell cycle arrest, and influenced the metastatic behavior of melanoma cells by decreasing migration, invasion, and colony formation. Based on these findings, it is believed that compound **6b** may represent an interesting scaffold to be explored toward the development of new antimelanoma agents.

Keywords: cinnamides, cinnamates, cinnamic acid, 1,2,3-triazoles, B16-F10 cell line

Introduction

Melanoma is the most serious type of skin cancer.^{1,2} It is originated from uncontrolled growth of melanocytes that are dendritic-like cells responsible for skin pigmentation.^{3,4} Melanoma accounts for the highest number of skin cancer deaths worldwide, and its incidence rate is increasing over the last years.⁵⁻⁷ In 2020, new melanoma cases in the United States were estimated to be about 100,350 with 6,850 deaths, whereas in Brazil approximately 8,450 new cases were projected.^{5,8}

Genetic mutations, excessive ultraviolet radiation exposure, severe sunburn, outdoor training, advanced age, and gender are relevant factors related to melanoma susceptibility.^{2,9} Additionally, melanoma has a high tendency to spread to other parts of the body. This metastatic behavior increases the challenge to treat this disease. Altogether, these facts evidence the melanoma severity.¹⁰⁻¹³

Surgical resection is the main option available for patients with early stage of melanoma. Once present the metastatic form, systemic treatment is the mainstay of therapy, which includes radiotherapy, cytotoxic chemotherapy, immunotherapy, and targeted therapies.^{5,12} Particularly, the chemotherapy has been using several compounds over the years, such as dacarbazine, dabrafenibe, binimetinib, vemurafenib, encorafenib, trametinib, and cobimetinib.^{12,14-18} However, these drugs still exhibit important side effects and low efficacy when used individually.¹⁹ These facts justify the need for the development of new chemotherapeutic agents to be used in the treatment of metastatic melanoma.

In the search for new antimelanoma agents, natural products have been an extraordinary source of compounds with great chemical variability and biological activities,²⁰⁻²³ including antimelanoma.^{24,25} Newman and Cragg²⁶ reported that 83% of anticancer drugs approved between 1981 and 2014 were either natural products *per se* or were based thereon. For instance, paclitaxel is an antimelanoma drug from natural sources derived from the bark of the Pacific yew tree (*Taxus brevifolia*).¹²

*e-mail: rossimiriam@ufmg.br

[#]These authors contributed equally to this work.

Cinnamic acid and its derivatives are natural plant-derived compounds that present antitumor and other biological activities. They have been used as templates for designing and arriving at newly compounds with antitumor activities.^{27,28} Our research group reported the preparation of a series of twenty-six cinnamic acid derivatives resulting from the connection of cinnamic acid with 1,2,3-triazole functionalities.²⁸ In the latter, B16-F10 cell line was used in *in vitro* assays to evaluate the antimelanoma activity of these compounds. The most potent cinnamate 3-(1-benzyl-1*H*-1,2,3-triazol-4-yl)propyl showed significant antiproliferative and antimetastatic activities against B16-F10 cells by interacting with matrix metalloproteinase 9 (MMP-9) and MMP-2, which are directly involved in melanoma progression.²⁸ Indeed, compounds bearing the 1,2,3-triazole ring present a variety of therapeutic effects including antitumor activity.^{29,30} Due to this fact, this fragment is relevant to medicinal chemistry²⁹ and used as pharmacophore.³¹ Likewise, cinnamides are cinnamic acid derivatives found in nature.³²⁻³⁴ Also known as cinnamamides and cinnamic acid amides, they present a broad range of pharmacological activities, which include antitubercular, anti-trypanosomal, anti-diabetic, anti-microbial, antiviral, anti-inflammatory, anti-malarial, nervous disorders, and antitumor.³⁵

In our ongoing efforts to find useful compounds for the treatment of melanoma,^{28,36,37} and considering antitumor activity linked to cinnamides, cinnamates, and compounds displaying the 1,2,3-triazole functionality, it is herein described the synthesis and antimelanoma evaluation of a series novel cinnamides and a bis cinnamate bearing 1,2,3-triazole fragment(s).

Results and Discussion

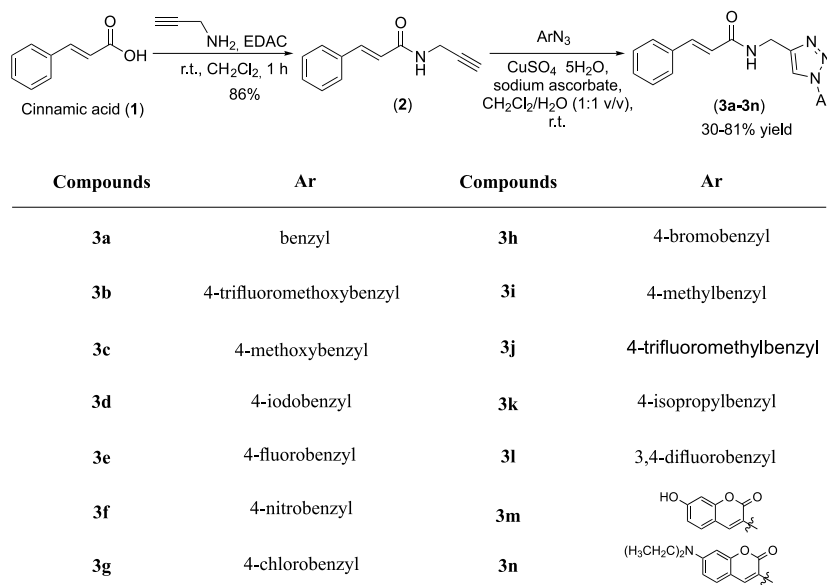
Synthesis

The steps involved in the synthesis of cinnamides **3a-3n** are outlined in Scheme 1.

The amide **2** was prepared via the reaction of cinnamic acid (**1**) and propargyl amine.³⁸ The reaction was carried out in the presence of EDAC (hydrochloride of 1-ethyl-3-(3'-dimethylaminopropyl)carbodiimide) which promoted coupling of the acid and the amine in good yield (86%). Then, the copper(I)-catalyzed alkyne-azide cycloaddition (CuAAC) reactions³⁹⁻⁴² between **2** and several aromatic azides afforded the cinnamides **3a-3n** with yields ranging from 30-81%.

The synthesis of cinnamides **3a-3n** required the preparation of twelve benzyl azides and two 3-azidocoumarins. The benzyl azides were prepared via conversion of benzyl alcohols to the corresponding ester sulfonates, followed by the treatment of these esters with sodium azide, as previously reported.⁴³ The 3-azidocoumarins, in turn, were obtained from the substituted salicylaldehyde and *N*-acetyl glycine or ethyl nitroacetate through routes involving two and three steps, according to methodology previously described.⁴⁴

One aspect deserves comment at this point. In our previous work, we synthesized a series of cinnamates bearing 1,2,3-triazole functionalities.²⁸ Indeed, these cinnamates presented different degrees of efficiency against the melanoma B16-F10 cell line. Their efficiency depended on the benzyl groups present in the triazole functionality of the cinnamates. These benzyl groups, in

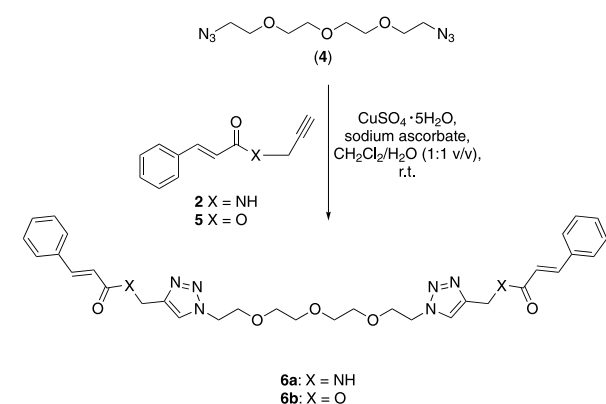


Scheme 1. Synthesis of cinnamides **3a-3n**.

turn, came from the benzyl azides. Herein, benzyl azides were also used in the preparation of cinnamides in order to make possible a comparison between the antimelanoma activity of cinnamates previously published by us²⁸ and the cinnamides herein investigated.

The structures of the new cinnamides **3a-3n** were confirmed based on infrared (IR), ¹H, ¹³C nuclear magnetic resonance (NMR) spectroscopic techniques and high-resolution mass spectrometry (HRMS) analyses. The IR spectrum showed bands for the N–H stretching within the 3230–3279 cm⁻¹ range. Also, carbonyl stretching vibrations for the amide groups were noticed within the interval 1615–1670 cm⁻¹. In the ¹H NMR, the coupling constants for the hydrogens of aliphatic double bonds were approximately equal to 16 Hz, which confirms the *trans* stereochemistry of these bonds. The singlet typically observed around 8 ppm confirmed the presence of the 1,2,3-triazole functionality in the structures of the cinnamides. The presence of the amide group was also confirmed by ¹³C NMR; the signals for the carbonyl groups of this functionality were noticed within the 164.8–168.4 ppm range. The molecular formulas of the cinnamides were confirmed via HRMS analyses.

Our research group has demonstrated important cytotoxic effects for symmetrical 1,4-disubstituted bis-1,2,3-triazoles.⁴⁵ Based on that, we decided to prepare the bis cinnamide **6a** and cinnamate **6b** as shown in Scheme 2. The synthesis of bis azide **4** has been previously reported.⁴⁵



Scheme 2. Preparation of compounds **6a** and **6b**.

The compound **6b** was prepared to compare the biological response of the bis ester cinnamate in relation to bis cinnamide **6a** (Scheme 2). The ester **5** was prepared via condensation of cinnamic acid (**1**) and propargyl alcohol promoted by EDAC as previously published by us.²⁸

The spectroscopic data that confirmed the structures of cinnamic acid derivatives **3a-3n**, **6a** and **6b** are available in the Supplementary Information (SI) section.

Effect of compounds **3a-3n**, **6a** and **6b** on the viability and cytotoxicity of B16-F10 cells

In the current study, compounds **3c**, **3e**, **3f**, **3j**, and **6b** reduced significantly the viability of metastatic B16-F10 cells at 100 μM (Figure 1). Therefore, these five compounds were evaluated for the half-maximal inhibitory concentration (IC₅₀). While compound **3c** presents an electron-donating group (–OCH₃) at the *para* position of the benzyl group, the compounds **3e** (–F), **3f** (–NO₂), and **3j** (–CF₃) have electron withdrawing ones. Besides, compound **6b** is a bis 1,2,3-triazole, a class of compounds endowed with antitumor activity.⁴⁵ While the similar 1,2,3-triazolic cinnamate with a *p*-methoxy benzyl group, at the 100.0 μM , was inactive against B16-F10 cell line,²⁸ the cinnamide **3c** could reduce cell viability in approximately 40%. On the contrary, the 1,2,3-triazolic cinnamates possessing the *p*-fluoro benzyl, *p*-nitro benzyl, and *p*-trifluoromethyl benzyl groups were equipotent to the cinnamides **3e**, **3f**, and **3j** counterparts.

Although metastatic B16-F10 is known to be very resistant to antitumor agents,⁴⁶ the compounds **3j** and **6b** displayed superior cytotoxic activity (IC₅₀ values of 153.4 and 57.66 μM , respectively) than cinnamic acid (> 200.0 μM , data not shown). In contrast, the cinnamides **3c**, **3e**, and **3f** showed IC₅₀ values greater than 200.0 μM . The cytotoxic effects presented by compounds **3j** and **6b** corroborate with previous studies, in which cinnamic acid derivatives also have presented relevant cytotoxic effects on the metastatic melanoma cell line.^{28,47} In the study of Sova *et al.*⁴⁷ cytotoxic effects of representative cinnamic acid esters and amides were seen in different types of cancer *in vitro*, including melanoma. Besides that, the compounds tested showed selectivity of these cytotoxic effects on the malignant cell lines *versus* the peripheral blood mononuclear cells.⁴⁷

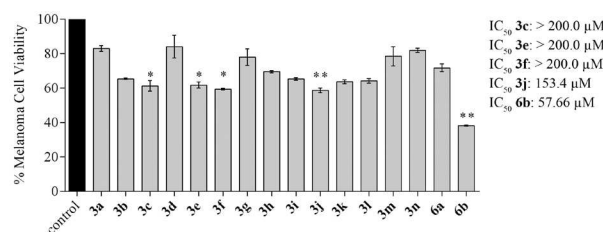


Figure 1. Effect of compounds **3a-3n**, **6a** and **6b** on cell viability of melanoma cells. B16-F10 metastatic melanoma was treated with 100.0 μM of each compound for 48 h. Each bar shows the mean of percentage of survival of melanoma cells determined by MTT (3-(4,5-dimethylthiazol-2-yl)-2,5-diphenyltetrazolium bromide) assay. The compounds that showed statistical difference in relation to the control were selected for IC₅₀ evaluation. Data expressed as the mean \pm SEM (standard error of the mean). **p* < 0.05 and ***p* < 0.01 *versus* control (DMSO, dimethyl sulfoxide, 0.4% v/v) by one-way ANOVA and Dunn's post-hoc test.

Effect of the compounds **3c**, **3e**, **3f**, **3j**, and **6b** on non-tumoral cell viability

The cytotoxicity of compounds in non-tumoral cells was also evaluated by means of Vero fibroblast-like kidney cells treated with the compounds **3c**, **3e**, **3f**, **3j**, and **6b**. Vero cells showed sensitivity for the compounds **3e**, **3f**, and **6b** at 100.0 μM , being **3e** the most cytotoxic (Figure 2).

This assay is relevant to compare the effect of compounds on non-tumoral cells, once that novel cancer chemotherapy relies on the selection of malignant-cell specific drugs and non-toxic to normal cells.⁴⁸ Meantime, cytotoxic chemotherapy can kill more cancer cells than normal tissue, as seen in cytotoxic drugs used to treat cancer.⁴⁹ It was the case of the results observed for the compound **6b**, which presented certain cytotoxicity in non-tumor cells, but it was the most effective in B16-F10 tumor cells. Taking the findings together, we selected the derivative **6b** for the subsequent assays due to its activity against the melanoma cell line B16-F10 (lowest IC_{50}).

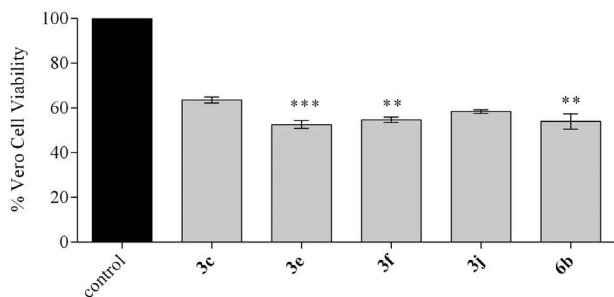


Figure 2. Effect of compounds **3c**, **3e**, **3f**, **3j** and **6b** on cell viability of non-tumor cell line. Vero fibroblast-like kidney cells were treated with 100.0 μM of each compound derived from cinnamic acid for 48 h. Each bar shows the mean of percentage of survival of Vero cells determined by MTT assay. Data expressed as the mean \pm SEM. ** $p < 0.01$ and *** $p < 0.001$ versus control (DMSO 0.4% v/v) by one-way ANOVA and Dunn's post-hoc test.

Effect of compound **6b** on the proliferation of melanoma cells

Cell proliferation was analyzed using the cell cycle assay. The compound **6b** induced a shift in the deoxyribonucleic acid (DNA) content of B16-F10 cells after 48 h incubation (Figure 3). Specifically, the percentage of cells in the G0/G1 phase was 75.40, 78.10, and 57.90% after incubation with compound **6b** at 12.5 ($p < 0.05$), 25.0 ($p < 0.05$), and 50.0 μM in contrast to the 45.43% of dimethyl sulfoxide (DMSO) control cells. Further, the percentage of cells in the S phase corresponded to 45.9% in the dimethyl sulfoxide (DMSO) control, and 21.7 ($p < 0.0001$), 14.3 ($p < 0.0001$), and 31.9% ($p < 0.01$) at 12.5, 25.0, and 50.0 μM . For the G2/M phase, the percentages were 8.70 (DMSO control), 2.86 (at 12.5 μM ; $p < 0.0001$), 7.64 (at 25.0 μM), and

10.31% (at 50.0 μM ; $p < 0.01$). Thus, these data expressed a B16-F10 cells accumulation in the G0/G1 phase and fewer cells in the S-phase (phase of duplication of genetic material), resulting in growth inhibition/cell cycle arrest. Drugs that affect the tumor cell cycle are promising, as they negatively influence the proliferation of cancer cells.⁵⁰ In the case of cinnamic acid derivatives, previous studies^{47,51} have reported their capacity to induce cell cycle arrest in cancer cells. Therefore, our data corroborate the studies with cinnamic acid derivatives, since the compounds inhibited cell proliferation by disruption of cell cycle.

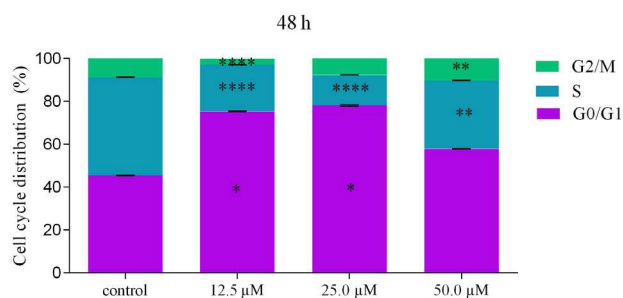


Figure 3. Effect of compound **6b** on melanoma cell cycle. B16-F10 cells were treated with 12.5, 25.0, and 50.0 μM of compound **6b**. Cells treated with DMSO 0.4% v/v were used as control. Cell cycle was evaluated using propidium iodide, followed by cytometry analysis after 48 h of incubation. Data expressed as the mean \pm SEM. * $p < 0.05$, ** $p < 0.01$ and *** $p < 0.0001$ versus control (DMSO 0.4% v/v) by one-way ANOVA and Dunnett's post-hoc test.

Effect of compound **6b** on the metastatic behavior of melanoma cells

Metastasis involves a series of progressive stages which include cell migration, invasion of blood and lymph vessels, cell colonization, and the ability of these cells to survive in other organs.^{52,53} In order to analyze the cell migration, we evaluated the cell migration capacity through the wound healing assay using concentrations of 12.5, 25.0 and 50.0 μM of the compound **6b** for 24 h, all concentrations below the IC_{50} value. The compound **6b** significantly reduced in approximately 42% the cell migration at the concentration of 50.0 μM , in relation to the DMSO control (Figure 4).

Cinnamic acid and its derivatives normally interfere with cell dynamics, decreasing cell migration. Niero and Machado-Santelli⁵⁴ observed that the treatment with cinnamic acid on melanoma cells caused cytoskeleton disruption. Any change in the cell cytoskeleton interferes with cell locomotion, since these filaments are crucial for cell movement. Therefore, our data confirm the hypothesis that cinnamic acid derivatives interfere with cell migration.

Once that **6b** interfered with cell migration and cell invasion is a key step of metastasis, invasion assay was performed. B16-F10 cells were treated with 12.5, 25.0 and

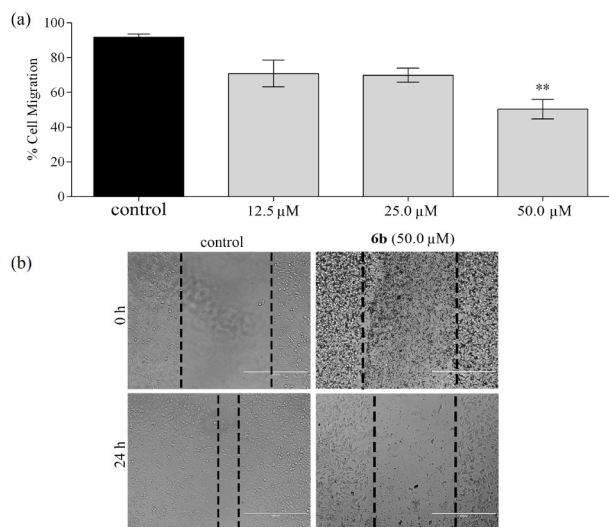


Figure 4. Effect of compound **6b** on migration of B16-F10 melanoma cells *in vitro*. (a) B16-F10 metastatic melanoma was wounded with a pipette tip and then treated with 12.5, 25.0 and 50.0 μM of **6b** compound for 24 h. (b) Photos of the wound were taken at 0 and 24 h after treatment with 50.0 μM of the compound under 100× magnification microscope. Data expressed as the mean ± SEM. ** $p < 0.01$ versus control (0.04% DMSO) by one-way ANOVA and Dunnett's post-hoc test.

50.0 μM of the compound **6b**. Cell invasion decreased after 24 h of treatment with compound **6b** at 12.5 (35.9%), 25.0 (44.3%), and 50.0 μM (58.7%) compared to vehicle-treated cells (DMSO 0.4% v/v) (Figure 5).

Compounds with properties to reduce cellular invasion of cancer cells are interesting.⁵⁵ The ability of these synthetic cinnamic acid derivatives to inhibit the invasive capacity of melanoma cells *in vitro*, shows once again that cinnamic acid and its derivatives have anti-invasive properties against cancer cells, an effect also observed against colon carcinoma cells, human lung, adenocarcinoma, and even against melanoma cells.^{28,56,57}

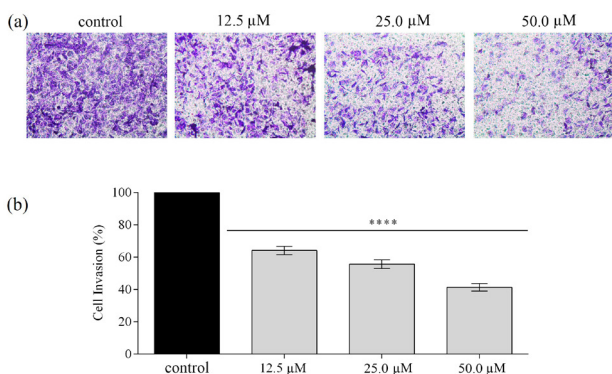


Figure 5. Effect of compound **6b** on invasion of B16-F10 melanoma cells *in vitro*. (a) Photomicrographs represent the cells invasion through matrigel-coated transwell. (b) The bar graph represents the percentage of invasive cell that was treated with 12.5, 25.0, and 50.0 μM of compound **6b** for 60 min. Data expressed as the mean ± SEM. **** $p < 0.0001$ versus control (DMSO 0.4% v/v) by one-way ANOVA and Dunnett's post-hoc test.

This anti-invasion action of compound **6b** may be related to the activity of metalloproteinases (MMPs), since previous studies^{28,56,57} have shown that cinnamic acid derivatives are potent inhibitors of MMPs.

Finally, the colony formation was also assessed to evaluate the long-term effects of the compound **6b**. This compound significantly reduced colony formation, with a reduction in the number of colonies at the concentrations of 12.5 (26.5%), 25.0 (41.6%) and 50.0 μM (53.3%) when compared to vehicle-treated cells (Figure 6). This important result is probably due to a set of factors, such as the negative action of compound **6b** on cell proliferation and its impact on cell mobility and invasion, as seen in previous *in vitro* assays.⁵⁸

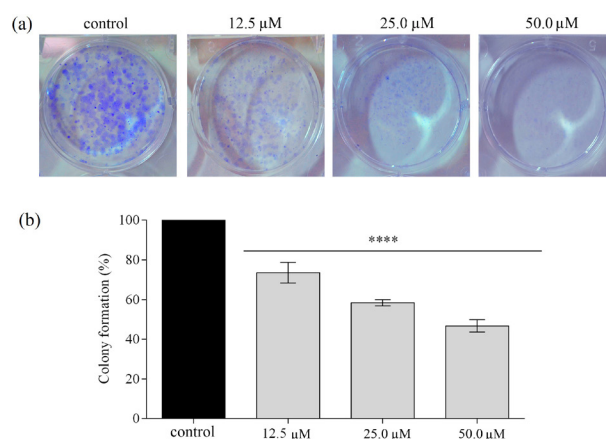


Figure 6. Effect of compound **6b** on colony formation of B16-F10 melanoma cells *in vitro*. (a) Photomicrographs showing the formation of B16-F10 colonies after treatment with 12.5, 25.0 and 50.0 μM of the compound **6b**. (b) The bar graph represents the percentage of colony formation after 7 days. Data expressed as mean ± SEM. **** $p < 0.0001$ versus control (DMSO 0.4% v/v) by one-way ANOVA and Dunnett's post-hoc test.

Taken together, all the *in vitro* experiments performed suggested that the cinnamic acid derivative would render antiproliferative and antimetastatic effect in melanoma cells.

Conclusions

In summary, a series of novel triazole cinnamides and a hitherto unknown bis-triazole ester cinnamate were prepared and had their antiproliferative and antimetastatic activities evaluated *in vitro* on B16-F10 murine cell line. It was demonstrated that the derivative **6b**, the most effective compound, reduced the melanoma cell viability, generated cell cycle arrest, and influenced the metastatic behavior of melanoma cells, by decreasing migration, invasion, and colony formation. Taken together, these results clearly showed the cytotoxic, antiproliferative and antimetastatic potential of compound **6b** against melanoma

cells and highlight the cinnamic acid derivative as possible therapeutic target for the treatment of metastatic cancers.

Experimental

Synthesis

Generalities

The solvents were purchased from Vetec (Rio de Janeiro, RJ, Brazil), Sigma-Aldrich (St. Louis, MO, US), and Synth (Diadema, São Paulo, Brazil) and were distilled before use. Distilled water was used in the experiments. The reagents were procured from Vetec (Rio de Janeiro, RJ, Brazil), Sigma-Aldrich (St. Louis, MO, US), Synth (Diadema, São Paulo, Brazil) and Oakwood Chemical (Estill, South Carolina, US) and used without further purification. The progress of the reactions was monitored by thin layer chromatography (TLC). For the purification of the reaction products, it was employed silica gel column chromatography (SiliCycle 0.035-0.070 mm, pore diameter 6 nm). The NMR spectra were recorded on Bruker (Billerica, Massachusetts, US) AVANCE DPX 200 MHz, AVANCE-III Onebay and Nanobay 400 MHz and AVANCE-NEO 600 MHz instruments, using CDCl₃, CD₃OD, or dimethyl sulfoxide (DMSO-*d*₆) as deuterated solvents. The ¹H NMR data are presented as follows: chemical shift (δ) in ppm, multiplicity, number of hydrogens, *J* values in hertz (Hz). Multiplicities are indicated by the following abbreviations: s (singlet), brs (broad singlet), d (doublet), dd (double of doublets), t (triplet), m (multiplet), q (quartet). For fluorine-containing derivatives, the multiplicity of some carbon signals are described along with *J* values in hertz. IR spectra were obtained using Varian 660-IR (Palo Alto, California, US) equipped with GladiATR scanning from 4000 to 500 cm⁻¹. Melting points were determined using a MQAPF-302 melting point apparatus (Microquímica, Santa Catarina, Brazil) and are uncorrected. High resolution mass spectra (HRMS) were obtained by electron spray ionization-mass spectrometry (ESI-MS) technique on a Q-Exactive (Thermo Scientific, Waltham, Massachusetts, United States of America) mass spectrometer and Solarix (Bruker Daltonics, Bremen, Germany) mass spectrometer. Details concerning the preparation of the intermediate compounds can be found in the SI section.

Synthesis of compounds **3a-3m** exemplified by the synthesis of *N*-((1-(4-benzyl-1*H*-1,2,3-triazol-4-yl)methyl)cinnamamide (**3a**)

To a 10.0 mL round-bottom flask, it was added azide (0.133 g, 1.00 mmol), water (2.00 mL), dichloromethane (2.00 mL), sodium ascorbate (39.6 mg, 0.200 mmol),

N-(prop-2-yn-1-yl)cinnamamide (**1**) (0.185 g, 1.00 mmol) and CuSO₄·5H₂O (0.100 g, 0.400 mmol). The reaction mixture was vigorously stirred at room temperature for 30 min. Subsequently, water (10.0 mL) was added and the resulting aqueous phase was extracted with dichloromethane (3 × 20.0 mL). The organic extracts were combined, and the resulting organic phase was dried over anhydrous Na₂SO₄, filtered, and concentrated under reduced pressure. The compound **5a** was purified from the residue by silica gel column chromatography eluted with hexane/ethyl acetate/methanol (5:3:1 v/v). The described procedure gave compound **5a** with 58% yield (0.185 g, 0.580 mmol). White solid; mp 165.8-166.9 °C; IR (ATR) ν_{\max} / cm⁻¹ 3229, 1614, 1565, 989, 729; ¹H NMR (400 MHz, DMSO-*d*₆) δ 4.41 (d, 2H, *J* 3.6 Hz), 5.55 (s, 2H), 6.63 (d, 1H, *J*_{trans} 16.0 Hz), 7.30-7.54 (m, 11 Hz), 8.00 (s, 1H), 8.57 (brs, 1H); ¹³C NMR (100 MHz, DMSO-*d*₆) δ 35.0, 53.4, 122.6, 123.7, 128.2, 128.7, 128.8, 129.4, 129.6, 130.2, 135.5, 136.8, 139.7, 145.7, 165.5; HRMS (ESI⁺) calcd. for C₁₉H₁₉N₄O [M + H]⁺: 319.1558, found: 319.1555.

Compounds **3b-3n** were prepared from the corresponding alkyne **2** and azides as described for compound **5a**. All the compounds were fully characterized by IR and NMR (¹H and ¹³C) as well as high resolution mass spectrometry. Structures of the compounds are supported by the following data.

N-((1-(4-(Trifluoromethoxy)benzyl)-1*H*-1,2,3-triazol-4-yl)methyl)cinnamamide (**3b**)

White solid, obtained in 53% yield; mp 194.0-194.8 °C; IR (ATR) ν_{\max} / cm⁻¹ 3247, 1649, 1598, 1538, 995; ¹H NMR (400 MHz, DMSO-*d*₆) δ 4.37 (d, 2H, *J* 5.6 Hz), 5.54 (s, 2H), 5.66 (s, 2H), 6.58 (d, 1H, *J*_{trans} 15.6 Hz), 7.25-7.39 (m, 8H), 7.45 (d, 2H, *J* 8.0 Hz), 7.99 (s, 1H), 8.53 (t, 1H, *J* 5.6 Hz); ¹³C NMR (100 MHz, DMSO-*d*₆) δ 35.0, 52.5, 122.0, 122.5, 123.8, 128.2, 129.6, 130.2, 130.7, 135.5, 136.2, 139.7, 145.8, 148.7, 165.6. The signal for the carbon of the CF₃ group was not observed. However, the remaining spectroscopic and spectrometric data confirmed the structure of the compound. HRMS (ESI⁺) calcd. for C₂₀H₁₇F₃N₄O₂Na [M + Na]⁺: 425.1201, found: 425.1196.

N-((1-(4-Methoxybenzyl)-1*H*-1,2,3-triazol-4-yl)methyl)cinnamamide (**3c**)

White solid, obtained in 41% yield; mp 162.5-163.2 °C; IR (ATR) ν_{\max} / cm⁻¹ 3235, 1649, 1609, 992; ¹H NMR (400 MHz, DMSO-*d*₆) δ 3.65 (s, 3H), 4.35 (d, 2H, *J* 5.6 Hz), 5.40 (s, 2H), 6.58 (d, 1H, *J*_{trans} 16 Hz), 6.84 (d, 2H, *J* 8.4 Hz), 7.22 (d, 2H, *J* 8.4 Hz), 7.28-7.34 (m, 3H), 7.38 (d, 1H, *J*_{trans} 16 Hz), 7.47 (d, 2H, *J* 7.6 Hz), 7.89 (s, 1H), 8.52 (t, 1H, *J* 5.6 Hz); ¹³C NMR (100 MHz, DMSO-*d*₆) δ 35.0, 53.0, 55.8, 114.8, 122.5, 123.4, 128.2, 128.7, 129.6, 130.2, 130.4,

135.5, 139.7, 145.6, 159.8, 165.6; HRMS (ESI⁺) calcd. for C₂₀H₂₁N₄O₂ [M + H]⁺: 349.1664, found: 349.1658.

N-((1-(4-Iodobenzyl)-1*H*-1,2,3-triazol-4-yl)methyl)cinnamamide (**3d**)

White solid, obtained in 69% yield; mp 208.2-209.6 °C; IR (ATR) ν_{\max} / cm⁻¹ 3257, 1650, 1606, 999, 750; ¹H NMR (400 MHz, DMSO-*d*₆) δ 4.33 (d, 2H, *J* 5.6 Hz), 5.43 (s, 2H), 6.55 (d, 1H, *J*_{trans} 16 Hz), 7.02 (d, 2H, *J* 8.0 Hz), 7.24-7.32 (m, 3H), 7.35 (d, 1H, *J*_{trans} 16 Hz), 7.44 (d, 2H, *J* 6.8 Hz), 7.63 (d, 2H, *J* 8.0 Hz), 7.91 (s, 1H), 8.50 (t, 1H, *J* 5.6 Hz); ¹³C NMR (100 MHz, DMSO-*d*₆) δ 35.0, 52.9, 95.0, 122.5, 123.8, 128.2, 129.6, 130.2, 131.0, 135.5, 136.5, 138.2, 139.8, 145.7, 165.6; HRMS (ESI⁺) calcd. for C₁₉H₁₈IN₄O [M + H]⁺: 445.05254, found: 445.05201.

N-((1-(4-Fluorobenzyl)-1*H*-1,2,3-triazol-4-yl)methyl)cinnamamide (**3e**)

White solid, obtained in 78% yield; mp 163.8-164.5 °C; IR (ATR) ν_{\max} / cm⁻¹ 3232, 1644, 1597, 1508, 992; ¹H NMR (600 MHz, DMSO-*d*₆) δ 4.44 (d, 2H, *J* 6.0 Hz), 5.57 (s, 2H), 6.66 (d, 2H, *J*_{trans} 15.6 Hz), 7.20 (t, 2H, *J* 8.7 Hz), 7.35-7.42 (m, 5H), 7.46 (d, 1H, *J*_{trans} 15.6 Hz), 7.55 (d, 2H, *J* 7.2 Hz), 8.03 (s, 1H), 8.60 (t, 1H, *J* 6.0 Hz); ¹³C NMR (150 MHz, DMSO-*d*₆) δ 34.8, 52.4, 116.0 (d, *J*_{C-F} 21.0 Hz), 122.3, 123.4, 128.0, 129.4, 130.0, 130.8 (d, *J*_{C-F} 8.4 Hz), 132.8 (d, *J*_{C-F} 3.3 Hz), 135.3, 139.5, 145.5, 162.4 (d, *J*_{C-F} 243 Hz), 165.3; HRMS (ESI⁺) calcd. for C₁₉H₁₈FN₄O [M + H]⁺: 337.14646, found: 337.14593.

N-((1-(4-Nitrobenzyl)-1*H*-1,2,3-triazol-4-yl)methyl)cinnamamide (**3f**)

Yellow solid, obtained in 66% yield; mp 184.4-186.1 °C; IR (ATR) ν_{\max} / cm⁻¹ 3353, 1649, 1610, 1518, 976, 723; ¹H NMR (400 MHz, DMSO-*d*₆) δ 4.45 (d, 2H, *J* 5.6 Hz), 5.77 (s, 2H), 6.66 (d, 1H, *J*_{trans} 16 Hz), 7.35-7.44 (m, 3H), 7.46 (d, 1H, *J*_{trans} 16 Hz), 7.53-7.56 (m, 4H), 8.11 (s, 1H), 8.24 (d, 2H, *J* 8.8 Hz), 8.63 (t, 1H, *J* 5.6 Hz); ¹³C NMR (100 MHz, DMSO-*d*₆) δ 34.8, 52.3, 122.4, 124.0, 124.4, 128.0, 129.4, 129.6, 130.0, 135.3, 139.5, 144.0, 145.7, 147.7, 165.6; HRMS (ESI⁺) calcd. for C₁₉H₁₈N₅O₃ [M + H]⁺: 364.14096, found: 364.14046.

N-((1-(4-Chlorobenzyl)-1*H*-1,2,3-triazol-4-yl)methyl)cinnamamide (**3g**)

White solid, obtained in 72% yield; mp 185.6-186.8 °C; IR (ATR) ν_{\max} / cm⁻¹ 3260, 1659, 1618, 972, 781; ¹H NMR (400 MHz, DMSO-*d*₆) δ 4.44 (d, 2H, *J* 5.5 Hz), 5.58 (s, 2H), 6.66 (d, 1H, *J*_{trans} 16 Hz), 7.34-7.46 (m, 8H), 7.56 (d, 2H, *J* 7.6 Hz), 8.04 (s, 1H), 8.60 (t, 1H, *J* 5.5 Hz); ¹³C NMR (100 MHz, DMSO-*d*₆) δ 34.8, 52.3, 122.4, 123.9,

124.4, 128.0, 129.4, 129.6, 129.7, 135.3, 139.5, 144.0, 145.7, 147.7, 165.4; HRMS (ESI⁺) calcd. for C₁₉H₁₈ClN₄O [M + H]⁺: 353.11691, found: 353.11642.

N-((1-(4-Bromobenzyl)-1*H*-1,2,3-triazol-4-yl)methyl)cinnamamide (**3h**)

White solid, obtained in 81% yield; mp 196.4-197.5 °C; IR (ATR) ν_{\max} / cm⁻¹ 3253, 1657, 1614, 1566, 971, 752; ¹H NMR (400 MHz, DMSO-*d*₆) δ 4.44 (d, 2H, *J* 5.6 Hz), 5.57 (s, 2H), 6.66 (d, 1H, *J*_{trans} 16.0 Hz), 7.29 (d, 2H, *J* 8.4 Hz), 7.37-7.44 (m, 3H), 7.46 (d, 1H, *J*_{trans} 16 Hz), 7.54-7.59 (m, 4H), 8.04 (s, 1H), 8.60 (t, 1H, *J* 5.6 Hz); ¹³C NMR (100 MHz, DMSO-*d*₆) δ 34.8, 52.5, 121.9, 122.4, 123.6, 128.0, 129.4, 130.0, 130.7, 132.1, 135.3, 136.0, 139.5, 145.5, 165.3; HRMS (ESI⁺) calcd. for C₁₉H₁₇BrN₄ONa [M + Na]⁺: 419.04834, found: 419.04788.

N-((1-(4-Methylbenzyl)-1*H*-1,2,3-triazol-4-yl)methyl)cinnamamide (**3i**)

White solid, obtained in 78% yield; mp 182.8-183.8 °C; IR (ATR) ν_{\max} / cm⁻¹ 3268, 1652, 1609, 1539, 988, 757; ¹H NMR (400 MHz, DMSO-*d*₆) δ 2.28 (s, 3H), 4.43 (d, 2H, *J* 5.6 Hz), 5.51 (s, 2H), 6.66 (d, 1H, *J*_{trans} 16 Hz), 7.17 (d, 2H, *J* 8 Hz), 7.23 (d, 2H, *J* 8 Hz), 7.16-7.24 (m, 4H), 7.36-7.41 (m, 3H), 7.46 (d, 1H, *J*_{trans} 16 Hz), 7.55 (d, 2H, *J* 6.4 Hz), 7.94 (s, 1H), 8.58 (t, 1H, *J* 5.6 Hz); ¹³C NMR (150 MHz, DMSO-*d*₆) δ 20.7, 34.4, 52.6, 121.9, 122.9, 127.6, 128.1, 129.0, 129.3, 129.5, 133.1, 134.9, 137.5, 139.1, 145.0, 164.9; HRMS (ESI⁺) calcd. for C₂₀H₂₁N₄O [M + H]⁺: 333.17154, found: 333.17104.

N-((1-(4-(Trifluoromethyl)benzyl)-1*H*-1,2,3-triazol-4-yl)methyl)cinnamamide (**3j**)

White solid, obtained in 71% yield; mp 214.1-215.3 °C; IR (ATR) ν_{\max} / cm⁻¹ 3253, 1649, 1602, 1112; ¹H NMR (400 MHz, DMSO-*d*₆) δ 4.45 (d, 2H, *J* 5.4 Hz), 5.71 (s, 2H), 6.67 (d, 1H, *J*_{trans} 16 Hz), 7.35-7.43 (m, 3H), 7.47 (d, 1H, *J*_{trans} 16 Hz), 7.51-7.56 (m, 4H), 7.75 (d, 2H, *J* 8.4 Hz), 8.10 (s, 1H), 8.62 (t, 1H, *J* 5.4 Hz); ¹³C NMR (100 MHz, DMSO-*d*₆) δ 34.8, 52.5, 122.4, 123.8, 126.1 (q, *J* 3.7 Hz), 128.0, 129.2, 129.4, 129.9, 135.3, 139.5, 141.2, 145.6, 165.4; HRMS (ESI⁺) calcd. for C₂₀H₁₈F₃N₄O [M + H]⁺: 387.14327, found: 387.14283.

N-((1-(4-Isopropylbenzyl)-1*H*-1,2,3-triazol-4-yl)methyl)cinnamamide (**3k**)

White solid, obtained in 72% yield; mp 199.1-200.5 °C; IR (ATR) ν_{\max} / cm⁻¹ 3279, 1653, 1610, 992; ¹H NMR (400 MHz, DMSO-*d*₆) δ 1.17 (d, 6H, *J* 6.9 Hz), 2.86 (septet, 1H, *J* 6.9 Hz), 4.42 (d, 2H, *J* 5.3 Hz), 5.52 (s, 2H), 6.65 (d, 1H, *J*_{trans} 16 Hz), 7.22-7.28 (m, 4H), 7.35-7.43 (m, 3H), 7.45

(d, 1H, J_{trans} 16 Hz), 7.55 (d, 2H, J 7.3 Hz), 8.01 (s, 1H), 8.59 (t, 1H, J 5.3 Hz); ^{13}C NMR (100 MHz, DMSO- d_6) δ 24.2, 33.6, 34.8, 53.0, 122.4, 123.4, 127.1, 128.0, 128.6, 129.4, 130.0, 134.0, 135.3, 139.5, 145.4, 148.9, 165.3; HRMS (ESI $^+$) calcd. for $\text{C}_{22}\text{H}_{25}\text{N}_4\text{O}$ [M + H] $^+$: 361.20284, found: 361.20230.

N-((1-(3,4-Difluorobenzyl)-1*H*-1,2,3-triazol-4-yl)methyl)cinnamamide (**3l**)

White solid, obtained in 77% yield; mp 149.3-150.8 °C; IR (ATR) ν_{max} / cm^{-1} 3241, 1518; ^1H NMR (400 MHz, DMSO- d_6) δ 4.43 (d, 2H, J 5.5 Hz), 5.57 (s, 2H), 6.65 (d, 1H, J_{trans} 16 Hz), 7.20 (s, 1H), 7.35-7.47 (m, 6H), 7.55 (d, 2H, J 6.9 Hz), 8.06 (s, 1H), 8.59 (t, 1H, J 5.5 Hz); ^{13}C NMR (100 MHz, DMSO- d_6) δ 34.3, 51.5, 117.3 (d, J 17.4 Hz), 117.8 (d, J 17.4 Hz), 121.8, 123.0, 125.1-125.2 (m), 127.4, 128.9, 129.4, 133.6-133.7 (m), 134.7, 139.0, 145.0, 147.9-148.0 (m), 150.3-150.5 (m), 164.8; HRMS (ESI $^+$) calcd. for $\text{C}_{19}\text{H}_{17}\text{F}_2\text{N}_4\text{O}$ [M + H] $^+$: 355.13704, found: 355.13663.

N-((1-(7-Hydroxy-2-oxo-2*H*-chromen-3-yl)-1*H*-1,2,3-triazol-4-yl)methyl)cinnamamide (**3m**)

White solid, obtained in 30% yield; mp 224.4-224.9 °C; IR (ATR) ν_{max} / cm^{-1} 3250, 3065, 1728, 1600; ^1H NMR (400 MHz, DMSO- d_6) δ 4.54 (d, 2H, J 5.2 Hz), 6.69 (d, 1H, J_{trans} 15.6 Hz), 6.85-6.92 (s, 2H, m), 7.36-7.44 (m, 3H), 7.49 (d, 1H, J_{trans} 15.6 Hz), 7.56 (d, 2H, J 6.9 Hz), 7.75 (d, 1H, J 8.5 Hz), 8.44 (s, 1H), 8.58 (s, 1H), 8.73 (t, 1H, J 5.2 Hz); ^{13}C NMR (100 MHz, DMSO- d_6) δ 34.7, 102.6, 110.8, 114.8, 119.8, 122.3, 124.3, 128.0, 129.4, 130.0, 131.4, 135.3, 136.6, 139.6, 145.5, 155.1, 156.8, 163.0, 165.5; HRMS (ESI $^+$) calcd. for $\text{C}_{19}\text{H}_{16}\text{F}_2\text{N}_4\text{ONa}$ [M + Na] $^+$: 411.10693, found: 411.10663.

N-((1-(7-(Diethylamino)-2-oxo-2*H*-chromen-3-yl)-1*H*-1,2,3-triazol-4-yl)methyl)cinnamamide (**3n**)

Yellow solid, obtained in 63% yield; mp 206.5-207.4 °C; IR (ATR) ν_{max} / cm^{-1} 3332, 1731, 1613, 968; ^1H NMR (400 MHz, DMSO- d_6) δ 1.13-1.47 (m, 6H), 3.46-3.51 (m, 4H), 4.53 (s, 2H), 6.66-6.71 (m, 2H), 6.82 (d, 1H, J 9.6 Hz), 7.40-7.42 (m, 3H), 7.48 (d, 1H, J_{trans} 16 Hz), 7.56-7.64 (m, 3H), 8.40 (s, 1H), 8.45 (s, 1H), 8.71 (s, 1H); ^{13}C NMR (100 MHz, DMSO- d_6) δ 12.5, 34.4, 44.4, 96.6, 106.7, 110.2, 116.5, 122.0, 123.9, 127.7, 129.1, 129.7, 130.7, 135.0, 136.7, 139.3, 145.0, 151.6, 155.8, 156.9, 165.1; HRMS (ESI $^+$) calcd. for $\text{C}_{25}\text{H}_{26}\text{N}_5\text{O}_3$ [M + H] $^+$: 444.20356, found: 444.20352.

Synthesis of (2*E*,2'*E*)-*N,N'*-((((oxybis(ethane-2,1-diyl))bis(oxy))bis(ethane-2,1-diyl))bis(1*H*-1,2,3-triazole-1,4-diyl))bis(methylene))bis(3-phenylacrylamide) (**6a**)

This compound was prepared via the reaction between

azide **4** and compound **2**, using the same methodology described for compound **3a**, however, 2.00 mmol of compound **2** was used for 1.00 mmol of azide **4**. A white solid was obtained in 34% yield, mp 152.4-153.5 °C; IR (ATR) ν_{max} / cm^{-1} 3266, 1667, 1629, 971; ^1H NMR (400 MHz, CD_3OD) δ 3.48-3.53 (m, 8H), 3.82 (t, 4H, J 5.2 Hz), 4.52 (t, 4H, J 5.2 Hz), 4.55 (s, 4H), 6.62 (d, 2H, J_{trans} 16 Hz), 7.35-7.39 (m, 6H), 7.52-7.58 (m, 6H), 7.92 (s, 2H); ^{13}C NMR (100 MHz, CD_3OD) δ 35.8, 51.4, 70.3, 71.5, 121.6, 125.1, 128.9, 130.0, 130.9, 136.2, 142.2, 146.0, 168.4; HRMS (ESI $^+$) calcd. for $\text{C}_{32}\text{H}_{38}\text{N}_8\text{O}_5\text{Na}$ [M + Na] $^+$: 637.28629, found: 637.28741.

(((Oxybis(ethane-2,1-diyl))bis(oxy))bis(ethane-2,1-diyl))bis(1*H*-1,2,3-triazole-1,4-diyl))bis(methylene) (2*E*,2'*E*)-bis(3-phenylacrylate) (**6b**)

This compound was obtained in 23% as colorless oil from the reaction of azide **4** and ester **5**, using the same methodology described for compound **6a**, IR (ATR) ν_{max} / cm^{-1} 3136, 1713, 1636, 1160; ^1H NMR (400 MHz, CDCl_3) δ 3.53-3.60 (m, 8H), 3.86 (t, 4H, J 5.1 Hz), 4.54 (t, 4H, J 5.1 Hz), 5.36 (s, 4H), 6.43 (d, 2H, J_{trans} 16.0 Hz), 7.36-7.39 (m, 6H), 7.48-7.51 (m, 4H), 7.70 (d, 2H, J_{trans} 16 Hz), 7.85 (s, 2H); ^{13}C NMR (100 MHz, CDCl_3) δ 50.4, 57.5, 69.3, 70.46, 70.54, 117.5, 125.11, 128.1, 128.9, 130.5, 134.2, 142.6, 145.6, 166.7; HRMS (ESI $^+$) calcd. for $\text{C}_{32}\text{H}_{37}\text{N}_6\text{O}_7$ [M + H] $^+$: 617.27237, found: 617.27271.

Cell culture

Murine melanoma cells (B16-F10) were kindly provided by Dr Mirian T. Paes Lopes (Department of Pharmacology, Universidade Federal de Minas Gerais, Belo Horizonte, Minas Gerais, Brazil). African green monkey kidney cell line (Vero) was kindly provided by Dr Juliana Lopes Rangel Fietto (Department of Biochemistry and Molecular Biology, Universidade Federal de Viçosa, Viçosa, Minas Gerais, Brazil). The cells were grown in Roswell Park Memorial Institute (RPMI-1640 medium Sigma-Aldrich, St. Louis, MO, US) supplemented with 10% (v/v) of fetal bovine serum (FBS) (LGC Biotecnologia, Cotia, Brazil), 100 g mL $^{-1}$ streptomycin, and 100 units mL $^{-1}$ penicillin at pH 7.2 and 37 °C under 5% CO_2 atmosphere.

Cell viability assay and cytotoxicity

B16-F10 cells were plated in 96-well at a concentration of 1.0×10^4 cells *per* well in a 96-well flat bottom microplate. The cells grew for 24 h and were treated with the concentration of 100 μM of each synthesized

compound derived from cinnamic acid **3a-3n**, **6a** and **6b**. DMSO (0.4% v/v) and RPMI-1640 were used as control. After 48 h of treatment, the cell viability was determined by MTT (3-(4,5 dimethylthiazol-2-yl)-2,5 diphenyltetrazolium bromide) (Sigma-Aldrich, St. Louis, MO, US) metabolization. The MTT solution was added to each well (final concentration 5 mg mL⁻¹) and the plate was incubated for 3 h. Finally, 100 µL of DMSO were added to each well and the absorbance was measured in a plate reader (Sinergy HT, Biotek) at 540 nm. Results were normalized considering the cultures treated with 0.4% DMSO (control). The half-maximal inhibitory concentration (IC₅₀) of the most active compounds was also analyzed using the MTT method, after treating the B16-F10 cells with increasing doses (0-200.0 µM) of these compounds. The IC₅₀ was calculated as previously reported.⁵⁹

Cell viability on non-tumor cell line

Vero cells, a non-tumor cell line, were plated at a concentration of 8.0 × 10⁴ cells *per* well in a 96-well flat bottom microplate. The cells grew for 24 h and were treated with the concentration of 100.0 µM of the five best compounds selected after the cell viability test in B16-F10. DMSO (0.4% v/v) and RPMI-1640 were used as control. After 48 h of treatment, the cell viability was determined by MTT Sigma-Aldrich (St. Louis, MO, US) metabolization. The MTT solution was added to each well (final concentration 5 mg mL⁻¹) and the plate was incubated for 3 h. Finally, 100 µL of DMSO was added to each well and the absorbance was measured in a plate reader (Sinergy HT, Biotek, Winooski, Vermont, USA) at 540 nm. Results were normalized considering the cultures treated with DMSO 0.4% v/v (control).

Cell cycle assay

B16-F10 cells were seeded on a 6-well plate at a density of 2.5 × 10⁵ cells *per* well and treated with compound **6b** at the concentrations of 12.5, 25.0, and 50.0 µM for 48 h. DMSO (0.4% v/v) was used as vehicle control. Then the cells were fixed in 70% ethanol, washed in phosphate-buffered saline (PBS), and incubated for 60 min in PBS containing propidium iodide (50 µg mL⁻¹, Sigma-Aldrich, St. Louis, MO, US) and RNase A (0.2 mg mL⁻¹, Invitrogen). The samples were analyzed by flow cytometry (FACS Verse, BD Bioscience, Franklanes, New Jersey, USA).

Cell migration assay

The wound-healing assay was conducted to evaluate the

ability of the compound **6b** to inhibit cell migration. B16-F10 cells were seeded onto 24-well plate at a concentration of 1.0 × 10⁵ cells *per* well and allowed to reach full confluence after incubation overnight at 37 °C under 5% CO₂ atmosphere. Monolayers were then wounded using a sterile 200 µL pipette tip. Cells were washed twice with PBS to remove detached cells and then treated with the compounds at the concentrations of 12.5, 25.0 and 50.0 µM. The DMSO vehicle treatment (0.4% v/v) was used as control. Photos of the wound were taken using an inverted microscope (Life Technologies, Carlsbad, California, USA). Wound closure rates were then calculated quantitatively as the difference between wound width at 0 and 24 h. Results were expressed as a percentage of cell migration.

Cell invasion assay

The matrigel matrix (BD Biosciences, Franklin Lakes, New Jersey, US) was diluted with serum-free RPMI-1640 culture medium at 1:12 ratio. Subsequently, the upper chamber of the transwell (8.0 µm polycarbonate membrane, Corning) was coated with 35 µL diluted Matrigel matrix and incubated at 37 °C, for 2 h, for full condensation. Then, the B16-F10 cells were re-suspended with serum-free RPMI-1640, treated with **6b** at 12.5, 25.0, and 50.0 µM for 60 min, and inoculated into the upper chamber Matrigel-precoated (5.0 × 10⁴ cells, 100 µL *per* well). The DMSO-vehicle treatment (0.4% v/v) was used as control. The well was filled with 650 µL of culture medium containing 10% v/v FBS as a chemoattractant. After 24 h, the chambers were fixed in methanol for 30 min, washed and stained with toluidine blue (1% v/v, Sigma-Aldrich, St. Louis, MO, US) for 15 min. Images from 10 fields were chosen at random/group, captured using an inverted microscope (Leica Microsystems, Wetzlar, Germany) and the cells were counted using the ImageJ software.⁶⁰ The results were expressed as a percentage of cell invasion.

Cell colony assay

B16-F10 cells were seeded in 6-well plates in triplicate at the density of 1.0 × 10³ cells *per* well. After 24 h, the cells were treated with the compound **6b** at 12.5, 25.0, and 50.0 µM for 24 h. The complete medium was exchanged for complete medium with 2% FBS, and the cells were cultured for 7 days. The colonies formed were then fixed and stained with toluidine blue solution (1% v/v, Sigma-Aldrich, St. Louis, MO, US) and methanol (20% v/v). Colonies were counted by using ImageJ software and the results were expressed as a percentage of the untreated control cultures.⁶⁰

Statistical analysis

All numeric data were obtained from three independent experiments, each experiment with triplicate, and are shown as mean \pm standard error of the mean (SEM). The analyses were performed using Microsoft Excel (Microsoft Office Software System) and GraphPad Prism (GraphPad Software Inc.).^{61,62} The statistical analyses were carried out by one-way analysis of variance (ANOVA) followed by Dunn's or Dunnett's tests. * $p < 0.05$, ** $p < 0.01$, *** $p < 0.001$ and **** $p < 0.0001$ were considered significant.

Supplementary Information

Supplementary data are available free of charge at <http://jbcbs.sbg.org.br> as PDF file.

Acknowledgments

We are grateful to FAPEMIG, CNPq, and CAPES for financial support.

Author Contributions

FSS was responsible for investigation, data curation, writing original draft and writing-review and editing; JAV was responsible for investigation, data curation and writing original draft; LSS performed acquisition of data; TBG performed acquisition of data; GDAL was responsible for biological experiments; LLO was responsible for data curation and formal analysis; MMN conducted the biological experiments; RRT was responsible for conceptualization, formal analysis, funding acquisition, writing original draft and supervision; RPF was responsible for planning, project administration, funding acquisition, writing-review and coordination.

References

- Bishop, J. A. N.; Jewell, R. In *Principles and Practice of Medical Genetics*, 6th ed.; Rimoin, D.; Pyeritz, R.; Korf, B., eds; Academic Press: Cambridge, UK, 2013.
- D'Orazio, J. A.; Jarrett, S.; Marsch, A.; Lagrew, J.; Clear, L.; In *Melanoma - Epidemiology, Genetics and Risk Factors*; Davids, L., ed.; IntechOpen: London, UK, 2013.
- Bandarchi, B.; Ma, L.; Navab, R.; Seth, A.; Rasty, G.; *Dermatol. Res. Pract.* **2010**, 2010, ID 583748.
- Cichorek, M.; Wachulska, M.; Stasiewicz, A.; Tyminska, A.; *Adv. Dermatol. Allergol.* **2013**, 30, 30.
- Cancer Facts & Figures 2020*. Available at <https://www.cancer.org/research/cancer-facts-statistics/all-cancer-facts-figures/cancer-facts-figures-2020.html>, accessed in July 2021.
- Apalla, Z.; Lallas, A.; Sotiriou, E.; Lazaridou, E.; Ioannides, D.; *Dermatol. Pract. Concept.* **2017**, 7, 1.
- Siegel, R. L.; Miller, K. D.; Jemal, A.; *Ca-Cancer J. Clin.* **2020**, 70, 7.
- de Oliveira Santos, M.; *Rev. Bras. Cancerol.* **2020**, 66, 1.
- Landi, M. T.; Bishop, D. T.; MacGregor, S.; Machiela, M. J.; Stratigos, A. J.; Ghiorzo, P.; Brossard, M.; Calista, D.; Choi, J.; Fargnoli, M. C.; Zhang, T.; Rodolfo, M.; Trower, A. J.; Menin, C.; Martinez, J.; Hadjisavvas, A.; Song, L.; Stefanaki, I.; Scolyer, R.; Yang, R.; Goldstein, A. M.; Potrony, M.; Kypreou, K. P.; Pastorino, L.; Queirolo, P.; Pellegrini, C.; Cattaneo, L.; Zawistowski, M.; Gimenez-Xavier, P.; Rodriguez, A.; Elefanti, L.; Manoukian, S.; Rivoltini, L.; Smith, B. H.; Loizidou, M. A.; Regno, L. D.; Massi, D.; Mandala, M.; Khosrotehrani, K.; Akslen, L. A.; Amos, L. A.; Andresen, P. A.; Avril, M.-F.; Azizi, M.-F.; Soyer, H. P.; Bataille, V.; Dalmasso, B.; Bowdler, L. M.; Burdon, K. P.; Chen, W. V.; Codd, V.; Craig, J. E.; Dębniak, T.; Falchi, M.; Fang, S.; Friedman, E.; Simi, S.; Galan, P.; Garcia-Casado, Z.; Gillanders, E. M.; Gordon, S.; Green, A.; Gruis, N. A.; Hansson, J.; Harland, M.; Harris, J.; Helsing, P.; Henders, A.; Marko Hočevár, V.; Höiom, D.; Hunter, C.; Ingvar, R.; Kumar, J.; Lang, Lathrop, G. M.; Lee, J. E.; Li, X.; Lubiński, J.; Mackie, R. M.; Malt, M.; Malvehy, J.; McAloney, H.; Mohamdi, K.; Molven, A.; Moses, E. K.; Neale, R. E.; Novaković, S.; Nyholt, D. R.; Olsson, H.; Orr, N.; Fritsche, L. G.; Puig-Butlle, J. A.; Qureshi, A. A.; Radford-Smith, G. L.; Randerson-Moor, J.; Requena, C.; Rowe, C.; Samani, N. J.; Sanna, M.; Schadendorf, D.; Schulze, H.-J.; Simms, L. A.; Smithers, M.; Song, F.; Swerdlow, A. J.; van der Stoep, N.; Kukutsch, N. A.; Visconti, A.; Wallace, L.; Ward, S. V.; Wheeler, L.; Sturm, R. A.; Hutchinson, A.; Jones, K.; Malasky, M.; Vogt, A.; Zhou, W.; Pooley, K. A.; Elder, D. E.; Han, J.; Hicks, B.; Hayward, N. K.; Kanetsky, P. A.; Brummett, C.; Montgomery, G. W.; Olsen, C. M.; Hayward, C.; Dunning, A. M.; Martin, N. G.; Evangelou, E.; Mann, G. J.; Long, G.; Pharoah, P. D. P.; Easton, D. F.; Barrett, J. H.; Cust, A. E.; Abecasis, G.; Duffy, D. L.; Whiteman, D. C.; Gogas, H.; de Nicolo, A.; Tucker, M. A.; Newton-Bishop, M. A.; *Nat. Genet.* **2020**, 52, 494.
- Maio, M. M.; Grob, J.-J.; Aamdal, S.; Bondarenko, I.; Robert, C.; Thomas, L.; Garbe, C. V. C.-S.; Testori, A.; Chen, T.-T.; Tschaike, M.; Walchok, J. D.; *J. Clin. Oncol.* **2015**, 33, 1191.
- Mattia, G.; Puglisi, R.; Ascione, B.; Malorni, W.; Carè, A.; Matarrese, P.; *Cell Death Discovery* **2018**, 25, 112.
- Bhatia, S.; Tykodi, S. S.; Thompson, J. A.; *Oncology* **2009**, 23, 488.
- Balch, C. M.; Buzaid, A. C.; Soong, S.-J.; Atkins, M. B.; Cascinelli, N.; Coit, D. G.; Fleming, I. D.; Gershenwald, J. E.; Houghton Jr., A.; Kirkwood, J. M.; McMasters, K. M.; Mihm, M. F.; Morton, D. L.; Reintgen, D. S.; Ross, M. I.; Sober, A.; Thompson, J. A.; Thompson, J. F.; *J. Clin. Oncol.* **2009**, 19, 3635.

14. Atallah, E.; Flaherty, L.; *Curr. Treat. Options Oncol.* **2005**, *6*, 185.
15. Domingues, B.; Lopes, J. M.; Soares, P.; Pópulo, H.; *ImmunoTargets Ther.* **2018**, *7*, 35.
16. Wróbel, S.; Przybyło, M.; Stepien, E.; *J. Clin. Med.* **2019**, *8*, 368.
17. National Cancer Institute; *Drugs Approved for Melanoma*, available at <https://www.cancer.gov/about-cancer/treatment/drugs/melanoma>, accessed in July 2021.
18. do Vale, J. A.; Lima, G. D. A.; Almeida, A. A.; Teixeira, R. R.; Neves, M. M. In *Horizons in Cancer Research*, vol. 77; Watanabe, H. S., ed.; Nova Science Publishers: Nova York, USA, 2020.
19. Gupta, A.; Gomes, F.; Lorigan, P.; *Melanoma Manage.* **2017**, *4*, 125.
20. Harvey, A. L.; *Drug Discovery Today* **2008**, *13*, 894.
21. Harvey, A. L.; Edrada-Ebel, R.; Quinn, R. J.; *Nat. Rev. Drug Discovery* **2015**, *14*, 111.
22. Thomford, N. E.; Senthebane, D. A.; Rowe, A.; Munro, D.; Seele, P.; Dzobo, A. M. K.; *Int. J. Mol. Sci.* **2018**, *19*, 1578.
23. Koparde, A. A.; Doijad, R. C.; Magdum, C. S.; In *Natural Products in Drug Discovery*; Intechopen: London, UK, 2019.
24. Chinembiri, T. N.; du Plessis, L. H.; Gerber, M.; Hamman, J. H.; du Plessis, J.; *Molecules* **2014**, *19*, 11679.
25. Alqathama, A.; Prieto, J. M.; *Nat. Prod. Rep.* **2015**, *32*, 1170.
26. Newman, D. J.; Cragg, G. M.; *J. Nat. Prod.* **2016**, *79*, 629.
27. De, P.; Baltas, M.; Bedos-Belval, F.; *Curr. Med. Chem.* **2011**, *18*, 1672.
28. Lima, G. D. A.; Rodrigues, M. P.; Mendes, T. A. O.; Moreira, G. A.; Siqueira, R. P.; da Silva, A. M.; Vaz, B. G.; Fietto, J. L. R.; Bressan, G. C.; Neves, M. M.; Teixeira, R. R.; *Toxicol. In Vitro* **2018**, *53*, 1.
29. Dheer, D.; Singhi, V.; Shankar, R.; *Bioorg. Chem.* **2017**, *71*, 30.
30. Agalave, S. G.; Maujan, S. R.; Pore, V. S.; *Chem. - Asian J.* **2011**, *6*, 2696.
31. Xu, Z.; Zhao, S.-J.; Liu, Y.; *Eur. J. Med. Chem.* **2019**, *183*, 111700.
32. Liu, X.; Luo, J.; Kong, L.; *Nat. Prod. Commun.* **2011**, *6*, 851.
33. de Araújo-Vilges, K. M.; de Oliveira, S. V.; Couto, S. C. P.; Fokoue, H. H.; Romero, G. A. S.; Kato, M. J.; Romeiro, L. A. S.; Leite, J. R. A.; Kuckelhaus, S. A. S.; *Pharm. Biol.* **2017**, *55*, 1601.
34. Phuwaspraisiran, P.; Puksasook, T.; Jong-Aramruang, J.; Kokpol, U.; *Bioorg. Med. Chem. Lett.* **2008**, *18*, 4956.
35. Gaikwad, N.; Nanduri, S.; Madhavi, Y. V.; *Eur. J. Med. Chem.* **2019**, *181*, 111561.
36. Moreira, G. A.; Lima, G. D. A.; Siqueira, R. P.; Barros, M. V. A.; Adjanooun, A. L. M.; Santos, V. C.; Barbosa, E. A. A.; Loterio, R. K.; de Paiva, J. C.; Gonçalves, V. H. S.; Viol, L. C. S.; Marques, E. S. A.; Júnior, A. S.; Almeida, M. R.; Fietto, J. L. R.; Neves, M. M.; Ferreira, R. S.; Teixeira, R. R.; Bressan, G. C.; *Toxicol. Appl. Pharmacol.* **2018**, *356*, 214.
37. do Vale, J. A.; de Souza, A. P. M.; Lima, G. D. A.; Gonçalves, V. H. S.; Moreira, G. A.; Barros, M. V. A.; Pereira, W. L.; Lazaroni e Merchid, N. C.; Fietto, J. L. R.; Bressan, G. C.; Teixeira, R. R.; Neves, M. M.; *Anticancer Drugs* **2020**, *31*, 718.
38. Neises, B.; Steglich, W.; *Angew. Chem., Int. Ed.* **1978**, *17*, 522.
39. Kolb, H. C.; Finn, M. G.; Sharpless, K. B.; *Angew. Chem., Int. Ed.* **2001**, *40*, 2004.
40. Rostovtsev, V. V.; Green, L. G.; Fokin, V. V.; Sharpless, K. B.; *Angew. Chem., Int. Ed.* **2002**, *41*, 2596.
41. Tornøe, C. W.; Christensen, C.; Meldal, M.; *J. Org. Chem.* **2002**, *67*, 3057.
42. Singh, M. S.; Chowdhury, S.; Koley, S.; *Tetrahedron* **2016**, *72*, 5257.
43. Borgati, T. F.; Alves, R. B.; Teixeira, R. R.; de Freitas, R. P.; Perdigo, T. G.; da Silva, S. F.; dos Santos, A. A.; Bastidas, A. J. O.; *J. Braz. Chem. Soc.* **2013**, *24*, 953.
44. Sivakumar, K.; Xie, F.; Cash, M.; Long, S.; Barnhill, H. N.; Wang, Q.; *Org. Lett.* **2004**, *24*, 4603.
45. Reis, W. J.; Moreira, P. O. L.; Alves, R. B.; Oliveira, H. H. M.; Silva, L. M.; Varotti, F. P.; Freitas, R. P.; *Curr. Top. Med. Chem.* **2018**, *18*, 1475.
46. Dunagin, M. C.; Torborg, S. R.; Torre, E. A.; Emert, B.; Krepler, C.; Beqiri, M.; Sproesser, K.; Brafford, P. A.; Xiao, M.; Eggen, E.; Anastopoulos, J. N.; Vargas-Garcia, C. A.; Singh, A.; Nathanson, K. L.; Herlyn, M.; Raj, A.; *Nature* **2017**, *546*, 431.
47. Sova, M.; Zizac, Z.; Stankovic, J. A. A.; Prijatelj, M.; Turk, S.; Jurani, Z. D.; Mlinari -Rascan, I.; Gobec, S.; *J. Med. Chem.* **2013**, *9*, 633.
48. Yang, Y.; Zhang, Y.; Li, N.; *J. Ethnopharmacol.* **2019**, *236*, 129.
49. Romaguera, J. E. In *Oncologic Imaging: A Multidisciplinary Approach*; Rohren, E. M.; Erasmus, J. J.; Szklaruk, J.; Vining, D.; Sandler, C. M.; Kaur, H.; Hagemester, F. B.; Madewell, J. E.; Raval, B.; Gladish, G., eds.; Elsevier Saunders: Philadelphia, USA, 2012.
50. Li, Y.; Zhang, G.; *Cancer Biol. Med.* **2017**, *14*, 348.
51. Hunke, M.; Martinez, W.; Kashyap, A.; Bokoskie, T.; Pattabiraman, M.; Chandra, S.; *Anticancer Res.* **2018**, *8*, 4469.
52. Gray-Schopfer, V.; Wellbrock, C.; Marais, R.; *Nature* **2007**, *445*, 851.
53. Balasas, T.; Callaghan, J.; Coombes, R. C.; Evans, J.; Hall, J. A.; Kinrade, S.; Jones, D.; Jones, P. S.; Jones, R.; Marshall, J. F.; Panico, M. B.; Shaw, J. A.; Steeg, P. S.; Sullivan, M.; Tong, W.; Westwell, A. D.; Ritchie, J. W. A.; *Nat. Rev.* **2019**, *16*, 185.
54. Niero, E. L. O.; Machado-Santelli, G. M.; *J. Exp. Clin. Cancer Res.* **2013**, *32*, 31.
55. Rosel, D.; Fernandes, M.; Veselý, P.; Heneberg, P.; Cermák, V.; Petruželka, L.; Kumar, S.; Sanz-Moreno, V.; Brábek, J.; *Trends Cancer* **2017**, *3*, 391.

56. Yen, G.-C.; Chen, Y.-L.; Sun, F.-M.; Chiang, Y.-L.; Lu, S.-H.; Weng, C.-J.; *Eur. J. Pharm. Sci.* **2011**, *44*, 281.
57. Tsai, C.-M.; Yen, G. C.; Sun, F. M.; Yang, S. F.; Weng, C. J.; *Mol. Pharmaceutics* **2013**, *10*, 1890.
58. Almeida, A. A.; Lima, G. D. A.; Eiterer, M.; Rodrigues, L. A.; do Vale, J. A.; Zanatta, A. C.; Bressan, G. C.; de Oliveira, L. L.; Leite, J. P. V.; *Planta Med.*, *in press*, DOI: 10.1055/a-1395-9046.
59. Siqueira, R. P.; Barbosa, E. A. A.; Polêto, M. D.; Righetto, G. L.; Seraphim, T. V.; Salgado, R. L.; Ferreira, J. G.; Barros, M. V. A.; de Oliveira, L. L.; Laranjeira, A. B. A.; Almeida, M. R.; Júnior, A. S.; Fietto, J. L. R.; Kobarg, J.; de Oliveira, E. B.; Teixeira, R. R.; Borges, J. C.; Yunes, J. A.; Bressan, G. C.; *PLoS One* **2015**, *10*, e0134882.
60. Rasband, W. S.; *ImageJ*, version 1.49; U. S. National Institutes of Health, Bethesda, Maryland, USA, 2015.
61. *Microsoft Excel*, version 16.0; Microsoft Company, Redmond, WA, USA, 2016.
62. *GraphPad Prism*, version 6.01; GraphPad Software, Inc.; Software Mackiey, San Diego, California, USA, 2012.

Submitted: May 31, 2021

Published online: August 3, 2021

